Opt Quant Electron (2016) 48:215
DOI 10.1007/s11082-016-0439-8

nBn HgCdTe infrared detector with HgTe(HgCdTe)/CdTe SLs barrier

D. Benyahia[1] · P. Martyniuk[1] · M. Kopytko[1] · J. Antoszewski[2] · W. Gawron[1] · P. Madejczyk[1] · J. Rutkowski[1] · R. Gu[2] · L. Faraone[2]

Received: 1 October 2015 / Accepted: 25 January 2016 / Published online: 29 February 2016

Abstract Several strategies have been implemented to improve the performance of infrared single pixel detectors at higher operating temperature condition. The most efficient and effective in HgCdTe technology are: non-equilibrium architectures and currently an idea of the barrier detector to include unipolar and complementary structures. Valence band offset between active layer and barrier impeding the minority carrier transport is considered to be the most important issue to overcome. Currently, implementation of the Cd composition and doping graded interfaces has been proposed. In this paper we present the performance (dark current, detectivity, time response) of the nBn detector with HgTe(HgCdTe)/CdTe superlattice barrier. The superlattice barrier is believed to decrease valence band offset between active and barrier layers. Theoretically estimated detectivity of mid-wave (cut-off wavelength, 4.8 μm) detector is $\sim 3\times 10^{12}$ cmHz$^{1/2}$/W and time response 150 ps for zero valence band offset, bias 2 V and temperature 155 K.

Keywords HOT · HgCdTe · BIRD · nBn · SLs HgTe(HgCdTe)/CdTe

This article is part of the Topical Collection on Numerical Simulation of Optoelectronic Devices, NUSOD' 15.

Guest Edited by Julien Javaloyes, Weida Hu, Slawek Sujecki and Yuh-Renn Wu.

✉ P. Martyniuk
pmartyniuk@wat.edu.pl; piotr.martyniuk@wat.edu.pl

[1] Institute of Applied Physics, Military University of Technology, 2 Kaliskiego Str., 00-908 Warsaw, Poland

[2] Microelectronics Research Group, The University of Western Australia, 35 Stirling Highway, Crawley 6009, Australia

1 Introduction

Currently, the infrared detector industry is dominated by mercury cadmium telluride (HgCdTe) detectors. A number of concepts to improve HgCdTe IR detectors' performance have been proposed, but significant improvement in reduction of the dark current has been reached by suppression of Auger thermal generation by implementing non-equilibrium conditions (Piotrowski and Rogalski 2004). In practice, most of HgCdTe $N^+p(\pi)P^+$ Auger suppressed photodiodes are based on complex, technologically difficult to grow graded gap and doping multi-layer structures (Ashley and Elliott 1985). A new strategy to achieve higher operating temperature (HOT) detectors includes the barrier structures (Maimon and Wicks 2006). Itsuno et al. presented nBn HgCdTe bulk device being a prospect for circumventing of the p-type doping problems in *molecular beam epitaxy* (MBE) technology (Itsuno et al. 2011). Valence band offset (VBO) between active layer and barrier blocking the minority carrier transport is considered to be the most important issue to overcome. Currently, implementation of the Cd composition and doping graded interfaces has been proposed (Akhavan et al. 2014, 2015). An alternate approach for reduction of the VBO is to use a HgTe(HgCdTe)/CdTe superlattice (SLs). HgTe(HgCdTe)/CdTe SLs have a type-III band alignment. Considered SLs is composed of alternating layers of HgTe(HgCdTe) and CdTe. The HgTe(HgCdTe) layers are the wells and the CdTe layers form the barriers for both types of carriers: electrons and holes. Band engineering capability may be introduced by incorporation of Hg into the barrier layers. The C1 and HH1 energy difference of SLs is controlled by the thicknesses of the HgTe(HgCdTe) well layers allowing fitting to the absorber layer in terms of VBO. The transport properties of carriers in HgTe(HgCdTe)/CdTe SLs are completely different in comparison to HgCdTe alloys, meaning that the SLs in-plane transport properties are noticeably different from those in the growth direction. The transport in the growth direction is of greatest importance for the device presented in this paper. The numerical simulations predict that the effective masses of electrons and holes can be tuned over a considerable range by varying the CdTe barrier layer widths. The effective mass of electrons is expected to exceed up to an order of magnitude the effective mass in alloys with the same bandgap reducing the tunneling currents by several orders of magnitude in the SLs-based detectors (Grein et al. 2006). In this paper we present the simulation of the dark current characteristics of the nBn barrier detector with HgTe(HgCdTe)/CdTe SLs barrier at $T = 155$ K for mid-wave infrared range (MWIR). The SLs barrier is believed to decrease VBO between active and barrier layers.

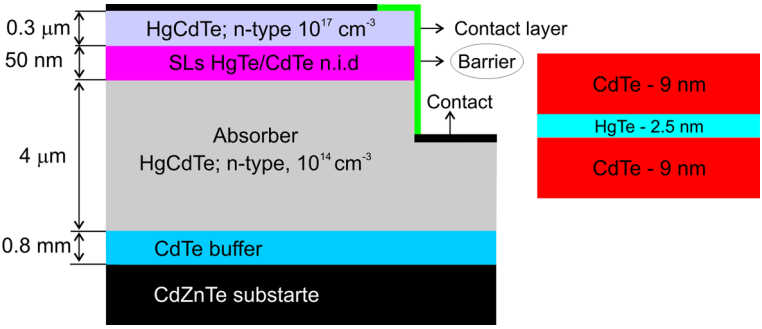

Fig. 1 Simulated nBn HgCdTe MWIR structure with HgTe(HgCdTe)/CdTe SLs barrier

Theoretically estimated detectivity of MWIR (cut-off wavelength, $\lambda_c = 4.8$ μm) detector is $\sim 3 \times 10^{12}$ cmHz$^{1/2}$/W and time response 150 ps for VBO = 0, bias 2 V and temperature, $T = 155$ K.

2 Simulation procedure

The device presented in this work were grown by MBE and fabricated in Microelectronics Research Group, The University of Western Australia. The schematic of a typical nBn detector structure with HgTe(HgCdTe)/CdTe SLs barrier design intended to operate in the MWIR (absorber layer Cd composition, $x = 0.3$, $T = 155$ K, cut-off wavelength, $\lambda_c = 4.8$ μm) spectral region is shown in Fig. 1. The detector structure was grown on a CdZnTe substrate and CdTe undopped buffer layers ($d = 0.8$ mm). The first layer of the devices was bulk absorber grown with a thickness of 4 μm and Cd composition 0.3, n-type doped with I ($n = 10^{14}$ cm^{-3}). Next the non-intentionally doped (n.i.d) HgTe(HgCdTe)/CdTe SLs (CdTe barrier $d = 9$ nm and HgTe well $d = 2.5$ nm) barrier layer was grown with a thickness of 50 nm. After the barrier layer a 0.3-μm thick bulk HgCdTe n-type contact doped with I ($n = 10^{17}$ cm^{-3}) was grown. The device diameter is 500 μm.

This heterostructure design was chosen to block the majority carriers (electrons) while the minority carriers can flow with no impedance due to an assumed lack of VBO between absorber and barrier layer. The barrier was found to be thick enough to prevent electron tunnelling between the top contact layer and active layer up to bias 4 V.

nBn HgCdTe with barrier HgTe(HgCdTe)/CdTe SLs detector was simulated with Apsys platform by Crosslight Inc. (Apsys 2015). The bulk based model was used in modeling of the device's transport properties. Theoretical modeling of the MWIR HgCdTe barrier detectors has been performed by numerical solving of the Poisson's equation and the carrier current continuity equations by the Newton–Richardson method. Ohmic contacts were modeled as Dirichlet boundary conditions—electron and hole quasi-Fermi levels are equal and assumed to be at the voltage of biased electrode, i.e., $E_{fn} = E_{fp} = V$. The applied model incorporates both HgCdTe bulk and barrier HgTe(HgCdTe)/CdTe electrical properties to estimate device performance taking into consideration radiative (RAD), Auger

Table 1 Parameters taken in modeling of SLs HgTe(HgCdTe)/CdTe in 8 × 8 kp (Yoo and Aggarwal 1989; Arriaga and Velasco 1992)

Parameter	HgTe(HgCdTe)	CdTe
E_g (eV) (bandgap)	−0.302; 0.22	1.6
Δ (eV) (spin–orbit coupling)	1.00	0.91
F (Kane parameter)	0.0	0.0
γ_1 (Luttinger parameter)	4.3675	1.540
$\gamma_2 = \gamma_3$ (Luttinger parameter)	1.034	0.015
a (eV) (hydrostatic deformation potential)	3.5	x
b (eV) (shear deformation potential)	−1.5	x
m^* (γ) (effective mass in the γ band)	0.026	0.087
C11 (Gpa) (elastic constant)	53.61	53.8
C12 (Gpa) (elastic constant)	36.6	37.4
C44 (Gpa) (elastic constant)	21.23	20.18
a (Å) (lattice constant)	6.462	6.482
c (%) (strain)	0.3	x

(AUG), Shockley Read-Hall (SRH) generation recombination (GR) mechanisms. RAD and AUG parameters for SLs layer were assumed to correspond to the bulk HgCdTe material with the same energy band gap (E_g). The carrier mobility dependence on bias was calculated in accordance with Canali (Beta) model (Turin 2005), while low field carrier mobility was assumed according to the paper by Scott (Scott 1972). The SLs was treated as an artificial material where C1 and HH1 effective masses were calculated using advanced 8 × 8 kp model in equilibrium condition incorporated in Apsys numerical platform. Affinity of HgTe(HgCdTe)/CdTe barrier was assumed 3.8 eV, while for HgCdTe absorber and contact layer 4.03 eV to reach zero VBO between barrier and absorber layer. The simulation parameters used for SLs HgTe(HgCdTe)/CdTe in 8 × 8 kp were presented in Table 1.

The calculated dispersion curves in growth direction for C1 and HH1 are presented in Fig. 2. The VBO between HgTe(HgCdTe) and CdTe was assumed 350 meV. The HgTe(HgCdTe)/CdTe SLs band gap energy was estimated at the level 548 meV. In growth direction effective masses were extracted from dispersion curves and assumed in the bulk based model, i.e. $m_e = 0.082\ m_0$ and $m_{hh} = 1.15\ m_0$ respectively.

Simple nBn structure requires that the valence bands of the three constituent layers line up closely to allow minority carrier transport between the absorber and contact layers. Band diagrams of the simulated structure for electron affinity calculated according the relation $\gamma = 4.23 - 0.813[E_g(x, T) - 0.083]$ and electron affinity corresponding to VBO = 0 are shown in Fig. 3a, b respectively. The band energy discontinuity of both barrier and absorber layers seems to be the most decisive parameter influencing performance of barrier structure. The barrier in conduction band (ΔE_c) is higher compared to barrier in valence band ($\Delta E_c > \Delta E_v$) [see Fig. 3]. At 400 mV, ΔE_v is ∼44 meV and $\Delta E_c \sim 238$ meV for electron affinity calculated with no correction ($A = 0$) while ΔE_v is 0 meV and $\Delta E_c \sim 282$ meV with extra component A (−50 meV) corresponding to VBO = 0. Dark and photocurrent are effectively blocked for ΔE_v; $\Delta E_c > 3k_B T \approx 39$ meV ($T = 155$ K, k_B—Boltzmann constant).

Measured and calculated dark current (I_{DARK}) and dynamic resistance (R_D) versus voltage are shown in Fig. 4. The calculations were performed assuming no intraband quantum tunneling transport mechanism through barrier (blue sold line) and with quantum tunnelling through barrier (pink dashed line). For a rectangular barrier, the tunneling

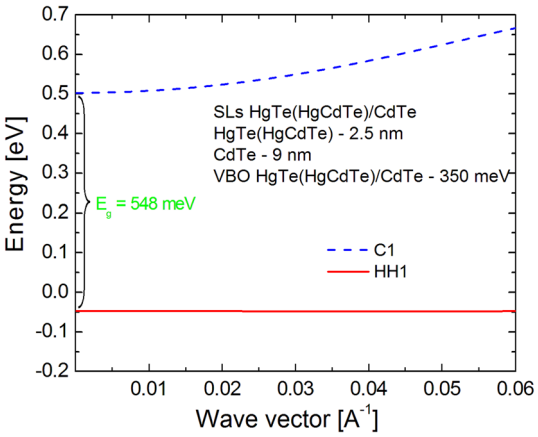

Fig. 2 Typical dispersion relation for C1 and HH1 in growth direction for HgTe(HgCdTe)/CdTe SLs at $T = 155$ K, VBO = 350 meV

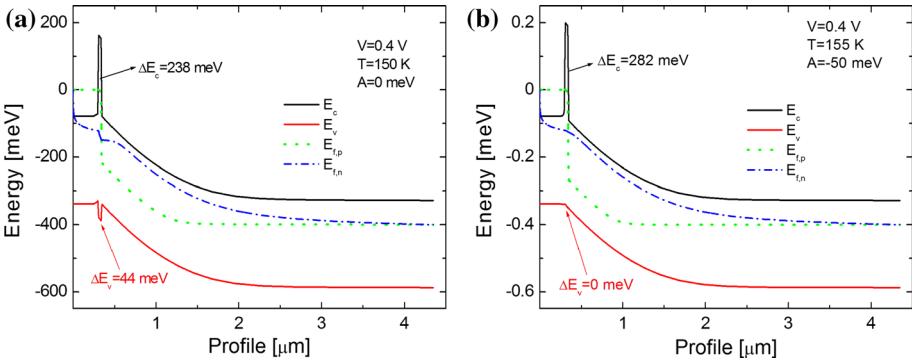

Fig. 3 Calculated energy band structures for nBn HgCdTe/B-SLs HgTe(HgCdTe)/CdTe for $V = 0.4$ V, $T = 150$ K: $A = 0$ meV (**a**); $A = -50$ meV (**b**)

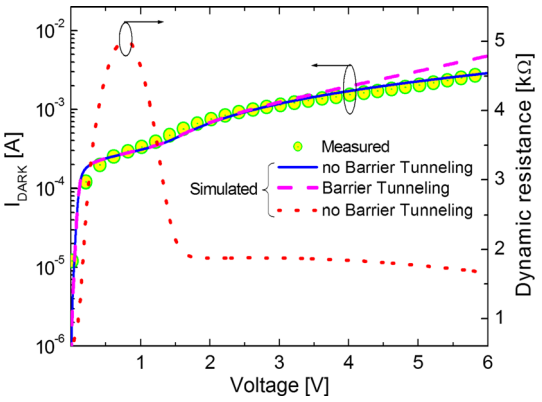

Fig. 4 I_{DARK} and R_D versus voltage for nBn detector with SLs HgTe(HgCdTe)/CdTe barrier at $T = 155$ K. (Color figure online)

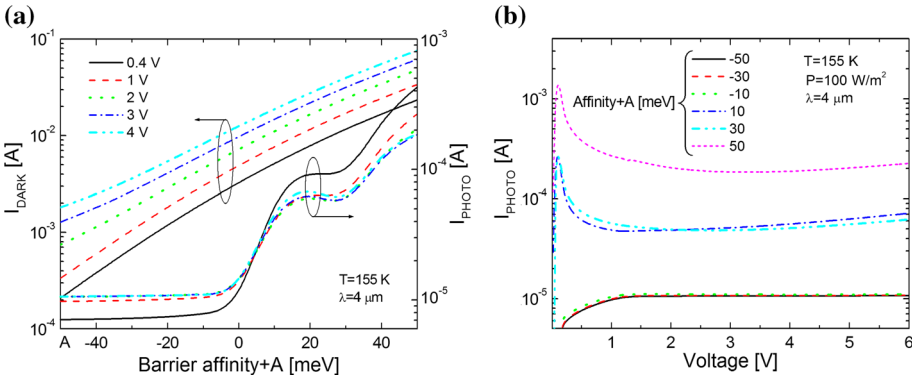

Fig. 5 Calculated dark and photocurrent versus barrier affinity for selected voltages 0.4–4 V (**a**); photocurrent versus voltage for selected affinity (**b**) for nBn HgCdTe/B-SLs HgTe(HgCdTe)/CdTe, $T = 155$ K

transparency was calculated with relation given by Yariv (1982). Oscillations in I_{DARK} characteristics in vicinity of 1 and 2 V are believed to be related to the dependence of energy barrier in conduction band (ΔE_c) versus voltage. For unbiased condition energy barrier in conduction band, $\Delta E_c \approx 300$ meV. It is shown that intraband quantum tunneling transport plays a decisive role for voltage >4 V.

Dark current and photocurrent (calculated for $\lambda = 4$ μm, power, $P = 100$ W/m^2) versus barrier electron affinity with extra correction A for selected voltages (0.4–4 V) are presented in Fig. 5a. Dark current increases sharply by three orders of magnitude within analyzed voltages which should be attributed to the lowering of the barrier in conduction band (ΔE_c) versus voltage. For $A < 0$ meV photocurrent stay constant ($\sim 10^{-5}$ A) and for $A > 0$ increases sharply due to the fact that energy barrier in conduction band decreases allowing unimpeded flow of the photogenerated carriers. The saturation range within A, 15–30 meV range is caused by the joint ratio of the ΔE_c and ΔE_v blocking and allowing unimpeded flow of the optically generated carriers. Detailed analysis of the photocurrent versus voltage for selected corrections A is shown in Fig. 5b.

The noise current was simulated using the following expression that includes both the thermal Johnson–Nyquist noise and electrical shot noise contributions:

$$i_n(V) = \sqrt{(4k_BT/R + 2qI_{DARK})}, \tag{1}$$

where R is the dynamic resistance area product, I_{DARK} is the dark current, and k_B is the Boltzmann constant. Detectivity (D^*) limited by thermal Johnson–Nyquist noise and electrical shot noise could be expressed by relation (where, R_i current responsivity and A is the area of the detector):

$$D^* = \frac{R_i}{i_n(V)}\sqrt{A}. \tag{2}$$

Calculated detectivity versus barrier affinity with extra correction A for selected voltages (0.4–4 V) is presented in Fig. 6a. For regular HgCdTe barrier ($A = 0$) detectivity is $\sim 10^{12}$ cmHz$^{1/2}$/W while for VBO = 0 ($A = -50$ meV), D^* reaches $\sim 4\times10^{12}$ cmHz$^{1/2}$/W. Increasing the ΔE_v and reducing ΔE_c assuming constant E_g allows to reach even $\sim 2\times10^{13}$ cmHz$^{1/2}$/W.

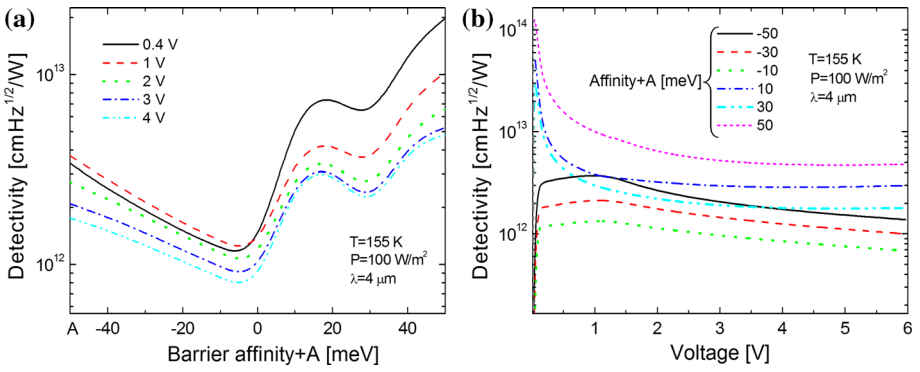

Fig. 6 Calculated detectivity versus barrier affinity for selected voltages 0.4–4 V (**a**); and versus voltage for selected affinities (**b**) for nBn HgCdTe/B-SLs HgTe(HgCdTe)/CdTe, $T = 155$ K

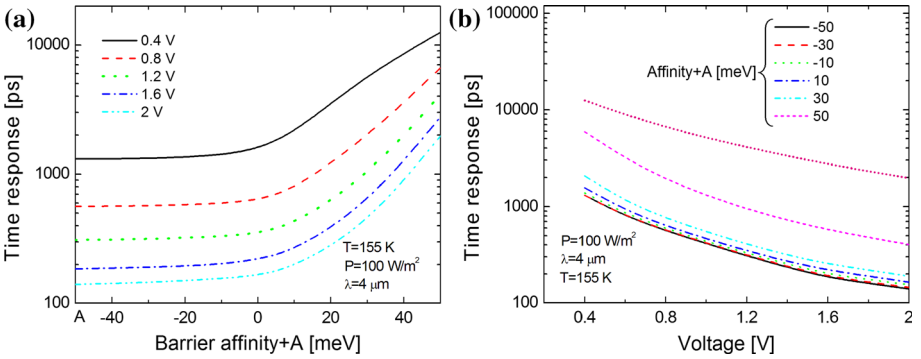

Fig. 7 Calculated time response versus barrier affinity for selected voltages 0.4–4 V (**a**); and versus voltage for selected affinities (**b**) for nBn HgCdTe/B-SLs HgTe(HgCdTe)/CdTe, $T = 155$ K

Time response (τ) characteristics versus affinity and voltage is presented in Fig. 7a, b. Time response strictly depends on minority carrier lifetime and drift time. For extra correction $A < 0$ meV, τ keeps constant reaching ~ 150 ps at 2 V corresponding to unimpeded hole transport to the contact. Once hole are blocked time response increases ($A > 0$) up to 1200 ps.

3 Conclusion

nBn detectors based on bulk HgCdTe naturally present a potential barrier in the valence band, which significantly reduces the performance. SLs HgTe(HgCdTe)/CdTe barrier gives an opportunity to reduce VBO in nBn structures leading to unimpeded transport of the photogenerated carriers to the contacts. Theoretically estimated detectivity of MWIR (4.8 μm) detector is $\sim 3 \times 10^{12}$ cmHz$^{1/2}$/W and time response 150 ps for zero valence band offset, bias 2 V and $T = 155$ K.

Acknowledgments This paper has been done under financial support of the Polish National Science Centre as the Research Projects: No. 2013/08/A/ST5/00773 and 2013/08/M/ST7/00913.

References

Akhavan, N.D., Umana-Membreno, G.A., Jolley, G., Antoszewski, J., Faraone, L.: A method of removing the valence band discontinuity in HgCdTe-based nBn detectors. Appl. Phys. Lett. **105**(12), 121110 (2014)

Akhavan, N.D., Jolley, G., Umana-Membreno, G., Jolley, G., Umana-Membreno, G.A., Antoszewski, J., Faraone, L.: Design of band engineered HgCdTe nBn detectors for MWIR and LWIR applications. IEEE Trans. Electron Dev. **62**(3), 722–728 (2015)

APSYS Macro/User's Manual ver. 2015. Crosslight Software, Inc. (2015)

Arriaga, J., Velasco, V.R.: Electronic properties of strained (001) HgTe-CdTe superlattices. Phys. Scr. **46**, 83–87 (1992)
Ashley, T., Elliott, C.T.: Non-equilibrium mode of operation for infrared detection. Electron. Lett. **21**, 451–452 (1985)
Grein, C.H., Boieriu, P., Flatté, M.E.: Single- and two-color HgTe/CdTe-superlattice based infrared detectors. Proc. SPIE **6127**, 61270W (2006)
Itsuno, A.M., Phillips, J.D., Velicu, S.: Design and modeling of HgCdTe nBn detectors. J. Electron. Mater. **40**(8), 1624–1629 (2011)
Maimon, S., Wicks, G.: nBn detector, an infrared detector with reduced dark current and higher operating temperature. Appl. Phys. Lett. **89**, 151109 (2006)
Piotrowski, J., Rogalski, A.: Uncooled long wavelength infrared photon detectors. Infrared Phys. Technol. **46**, 115–131 (2004)
Scott, W.: Electron mobility in $Hg_{1-x}Cd_xTe$. J. Appl. Phys. **43**, 1055–1062 (1972)
Turin, V.O.: A modified transferred-electron high-field mobility model for GaN devices simulation. Solid-State Electron. **49**, 1678–1682 (2005)
Wenus, J., Rutkowski, J., Rogalski, A.: Two-dimensional analysis of double-layer heterojunction HgCdTe Photodiodes. IEEE Trans. Electron Dev. **48**(7), 1326–1332 (2001)
Yariv, A.: An Introduction to Theory and Applications of Quantum Mechanics. Wiley, New York (1982)
Yoo, K.H., Aggarwal, R.L.: HgTe/CdTe superlattice band calculation with a transfer matrix method. JVST A **7**, 415–419 (1989)